BIO-BASED EPOXY RESINS AND COMPOSITES FROM EPOXIDIZED LINSEED OIL CROSSLINKED WITH DIFFERENT CYCLIC ANHYDRIDES AND THEIR COMBINATION WITH LIGNIN

ROXANA DINU and ALICE MIJA

Université Côte d'Azur, Institut de Chimie de Nice, UMR CNRS 7272,
28 Av. Valrose, 06108 Nice Cedex 02, France
✉ *Corresponding author: Alice Mija, Alice.Mija@univ-cotedazur.fr*

Dedicated to Academician Cristofor I. Simionescu,
on his 100th birth anniversary

Biobased resins and composites with high biobased carbon content were prepared and characterized. Epoxidized linseed oil (ELO) was copolymerized with four cyclic anhydrides, the initiation step being optimized in terms of initiator nature and its ratio. The optimized ELO/anhydride formulations were combined with a high load of lignin, as biofiller, ~30 wt%. The obtained materials were characterized by TGA, DSC, DMA, gel content, water absorption (WA) and Shore hardness tests. The results revealed very good thermomechanical properties, high gel content and low WA, opening the way to their utilization as a sustainable alternative to oil-based resins and composites.

INTRODUCTION

Plastics have become one of the most representative inventions in the evolution of the society, but their inadequate management has led to its conversion into a harmful and unfriendly factor for the environment. The first knowledge about the development and use of polymeric materials dates back to 1600 BC,[1] but their industrial production and use began in 1950, generating so far around 6.3 billion tons of plastic worldwide.[2] Both the continuous growth of the population and its needs, and the global pollution have led to an increased focus on the application and implementation of a sustainable economy.[3] For this purpose, intense researches are carried out for the replacement of fossil derivatives, which are a limited resource and environmentally unfriendly, with natural and renewable ones. Also, a continuous challenge in research is to find effective ways of converting bioresources into fuels and chemicals, and to design new innovative, green and environmentally friendly routes of developing, recovering and reusing polymeric materials.

Epoxy resins are some of the most important thermoset materials due to their excellent bonding property, high mechanical properties, and chemical resistance. In addition, epoxy resins can have different properties, because they can be combined and cured with various compounds, leading to their use in a wide range of fields, such as composites, adhesives, coatings, civil engineering, automotive sector and electrical materials.[4–6] Most of the industrially used epoxy monomers are obtained from petroleum-based resources, but in the last decades, alternative molecules have been produced and studied, as for example, those derived from vegetable oils. Generally, vegetable oils are renewable materials constituted by triglycerides formed from glycerol and fatty acids. The epoxidation of vegetable oils, such as soybean oil or linseed oil, is a most important and useful exploitation of double bonds functionalization, leading to the generation of bio-based monomers and resins able to replace those from fossil

derivatives, such as the diglycidyl ether of bisphenol A (DGEBA).[7]

Epoxidized linseed oil (ELO) is one of the compounds intensely investigated for the development of new resins and polymeric composites, due to its relatively high functional oxirane content.[8] For example, Boquillon *et al.*[9] developed thermoset polymeric networks based on ELO and dianhydride based curing agents. The influence of the dianhydride nature, but also of different types of catalysts, such as tertiary amines and imidazoles, on the curing mechanisms, the structure and the thermo-mechanical properties of the networks were investigated. Samper *et al.*[10] developed new polymeric resins feasible to use in the development of green composites. The polymeric materials were designed from epoxidized soybean oil (ESO), epoxidized linseed oil (ELO) and different mixtures of the two monomers, crosslinked with phthalic anhydride and maleic anhydride, using benzyl dimethyl amine as catalyst. Based on the physico-chemical and mechanical investigations, the optimal formulations were found to be those with ELO and with 80:20 ELO:ESO. Important studies have also been carried out by Di Mauro *et al.*[11–13] for a large series of epoxidized vegetable oils for the development of new polymeric resins with the capacity to be reprocessed and recycled, but also with physico-chemical and mechanical performances feasible for industrial use.

The most important renewable resource suitable for the development of new biopolymers and capable of replacing synthetic and petroleum-derived materials is biomass.[14–16] Lignocellulosic biomass consists of three important carbohydrates, such as cellulose (35-50%), hemicelluloses (20-35%) and lignin (10-25%).[17] Lignin is a three-dimensional amorphous phenolic polymer, whose structure is formed by three phenylpropanes building blocks, such as *p*-coumaryl alcohol, coniferyl alcohol, and sinapyl alcohol, connected through carbon-carbon and ether bonds.[18] Its function as cellular glue provides overall rigidity to the structure of plants and trees and resistance against insects and pathogens. Generally, softwoods contain more lignin than the hardwoods.[19] Lignin is still a by-product of chemical pulping processes, and its characteristic functional chemical groups are hydroxyl (phenolic and alcoholic), methoxy, carbonyl and carboxyl.[20,21] The annual lignin production is about 20 million tons worldwide, most of which is actually burned for energy.[15,22] In an attempt to valorise it for the development of new materials based on natural raw products, lignin has been used with various polymers, such as polypropylene,[23,24] poly(lactic acid),[25,26] polyvinyl chloride,[27] or different epoxies.[28–31] In our previous studies, lignin was used as filler in the development of composites, using bio-resins based on resorcinol diglycidyl ether,[32] or industrial by-products (humins from biorefineries) as polymeric matrices.[33]

The purpose of this work was the development of bio-based resins and composites using renewable, cost competitive and commercial compounds. Firstly, thermoset resins were developed based on epoxidized linseed oil crosslinked with four different anhydrides, the mixtures being initiated by 1-methylimidazole. Secondly, bio-based composites were produced using a very large amount of kraft lignin, about 30% by weight. As far as we know, ELO-based epoxy resins have so far not been combined and reinforced with lignin. The curing behaviour of the resins, but also the influence of lignin on the crosslinking reactivity was investigated by differential scanning calorimetry (DSC). The physical, thermal, and thermo-mechanical properties of the designed resins and composites were studied using different technics, such as TGA and DMA, as well as Shore D hardness, water absorption and gel content assessment, for their subsequent classification in an industrial application area.

EXPERIMENTAL

Materials

The epoxy materials were developed starting from a commercially available epoxidized linseed oil (ELO), supplied by Valtris Specialty Chemicals. This bio-based epoxy is a yellow viscous liquid (~1200 Pa.s), with an average molecular weight of about 980 $g.mol^{-1}$ and an average functionality of 5.5 epoxides per triglyceride. Different anhydrides, such as *cis*-1,2,3,6-tetrahydrophthalic anhydride (T; 95%), hexahydro-4-methylphthalic anhydride (H; mixture of *cis* and *trans*, 96%), (2-dodecen-1-yl)succinic anhydride (D; 95%), methyl nadic anhydride (M; ≥ 95.0%), were used as hardener, and 1-

methylimidazole (1-MIM; ≥99%) as initiator. These chemical products were purchased from Sigma-Aldrich (France) and used as received, without further purification. The fractionated Kraft lignin (Lig), supplied by VTT Technical Research Centre (Finland), was used as structural reinforcing agent. This natural compound is a brown powder with a sulphur content of about 1-3% and a pH ranging between 2.5-7. The molecular representations of the compounds used in the manufacturing process of the epoxy materials are exhibited in Figure 1.

Synthesis of crosslinked networks

To design the epoxy resins, the 1:1 stoichiometric ratio of the epoxy groups to the anhydride groups was used. The proper amount of ELO was heated at 70 °C to decrease its viscosity. Then, the required amount of anhydride was added to the epoxy compound, and the mixtures were vigorously mechanically stirred homogeneously for 10 min. To facilitate the reactions, 1-methylimidazole (1-MIM) was used as initiator, being added in the proportion of 3 wt%, based on the total weight of the curing agent-epoxy mixture. The homogenous blends were poured in silicon molds and introduced into a preheated convection oven for the curing and post-curing treatment.

The composite materials were developed by mechanically mixing the epoxy/anhydride stoichiometric blends with 30 wt% of kraft lignin, and after homogenization, 3 wt% initiator was added. To establish the optimum amount of filler, different percentages of lignin were tested by DSC, the crosslinking exothermic curves being displayed in Figure 2b. For complete curing of the resins and composites, the formulations were subjected to a two-stage curing process selected according to preliminary calorimetric DSC studies: 150 °C for 2 hours and then 180 °C for 1.5 hours.

Differential scanning calorimetry (DSC)

The crosslinking profile of the epoxy-based resins, but also the influence of the lignin on the curing reactivity, was examined using a DSC 3 Mettler Toledo apparatus. Approximately 5-10 mg of fresh samples were placed in 40 µL aluminium pans and scanned from 25 to 250 °C at a heating rate of 10 °C.min^{-1}. The onset (T_{onset}) and end curing (T_{end}) temperatures, the temperature at which the maximum crosslinking reaction takes place (T_{peak}), and the reaction enthalpy (ΔH) of the ELO-based resins and composite formulations were determined. The DSC technique was also used to investigate the glass transition, T_g, of the materials. Crosslinked samples of 12-17 mg were placed in 40 µL aluminium crucibles and subjected to a two heating-cooling cycle from -50 °C to 200 °C 10 °C.min^{-1}. The T_g values were recorded from the second cycle and defined as the temperature at the inflection point in the plot of heat flow *vs.* temperature DSC curves. All the DSC data were analyzed by STARe Software.

Thermogravimetric analysis (TGA)

The thermal stabilities were examined using a TGA 2 Mettler Toledo device. Cured samples, of 15 mg, were placed into 70 µL alumina crucibles and subjected to a heating program from 25 to 1000 °C, at 10 °C min^{-1}, in an oxidative atmosphere (50 mL.min^{-1}). The degradation temperature of the studied polymeric materials was recorded as the temperature at which the materials lose 5% of their mass ($T_{5\%}$).

Dynamic mechanical analysis (DMA)

The viscoelastic behavior of the resins and composites was studied using a DMA 1 Mettler Toledo. The specimens, with dimensions of about 50 × 8 × 4 mm^3 (length × width × thickness), were analyzed from -60 °C to 200 °C, at a heating rate of 3 °C.min^{-1}. The frequency and the amplitude were set at 1.0 Hz and 20 µm, respectively. The DMA experiments were performed using a three-point bending accessory, and the obtained data, such as storage modulus (E'), loss modulus (E''), and damping factor (tan $\delta = E'/E''$), were examined by STARe Software. To reduce the errors, each specimen was analyzed twice, the results being averaged.

Shore hardness tests

The hardness tests were carried out using a Shore D durometer (Zwick Roell 3116 Hardness Tester), in compliance with the standards: ISO 7619-1, ASTM D2240, and ISO 868. The stiffness of the resins and composites was determined applying a load force of 50 N ± 0.5 N, the values being recorded upon firm contact between the device presser foot and the analyzed sample. For greater accuracy, a minimum of six measurements were taken and the average values were calculated.

Water absorption

The water absorbed (WA) by the epoxy-based resins and the composites was investigated using the ASTM D570[34] standard test method, the obtained results being compared with those obtained using the DSC method. Firstly, rectangular samples (10 × 8 × 4 mm^3) were dried in an oven at 50 °C for 24 h, cooled in a desiccator, and then weighed (W_0) with a ML3002T Mettler Toledo precision balance. For the 24 h immersion procedure (ASTM D570 standard), the conditioned specimens were entirely immersed in distilled water at room temperature and maintained for 24 h. At the end of the 24 h, the tested samples were removed from the water, carefully wiped with filter paper and their mass was measured (W_t). The moisture content ratio (WA, %) was calculated using the equation:[34]

$$WA, \% = \frac{W_t - W_0}{W_0} \times 100 \quad (1)$$

where W_0 represents the conditioned weight of the tested sample and W_t is the wet mass of the tested sample after 24 h of immersion.

The WA was also determined by DSC. Samples of 5 mg, collected from the specimens analyzed by the prior procedure, were placed into 40 µL aluminium crucibles and subjected to a scan from 30 °C to 300 °C, at a heating rate of 10 °C.min^{-1}. Subsequently, the samples were tempered to ambient temperature, followed by a similar second heating program. The moisture content by DSC was calculated using the water evaporation heat of 2400 J.g^{-1}, and the obtained values were compared with the data achieved by ASTM D570 standard method.

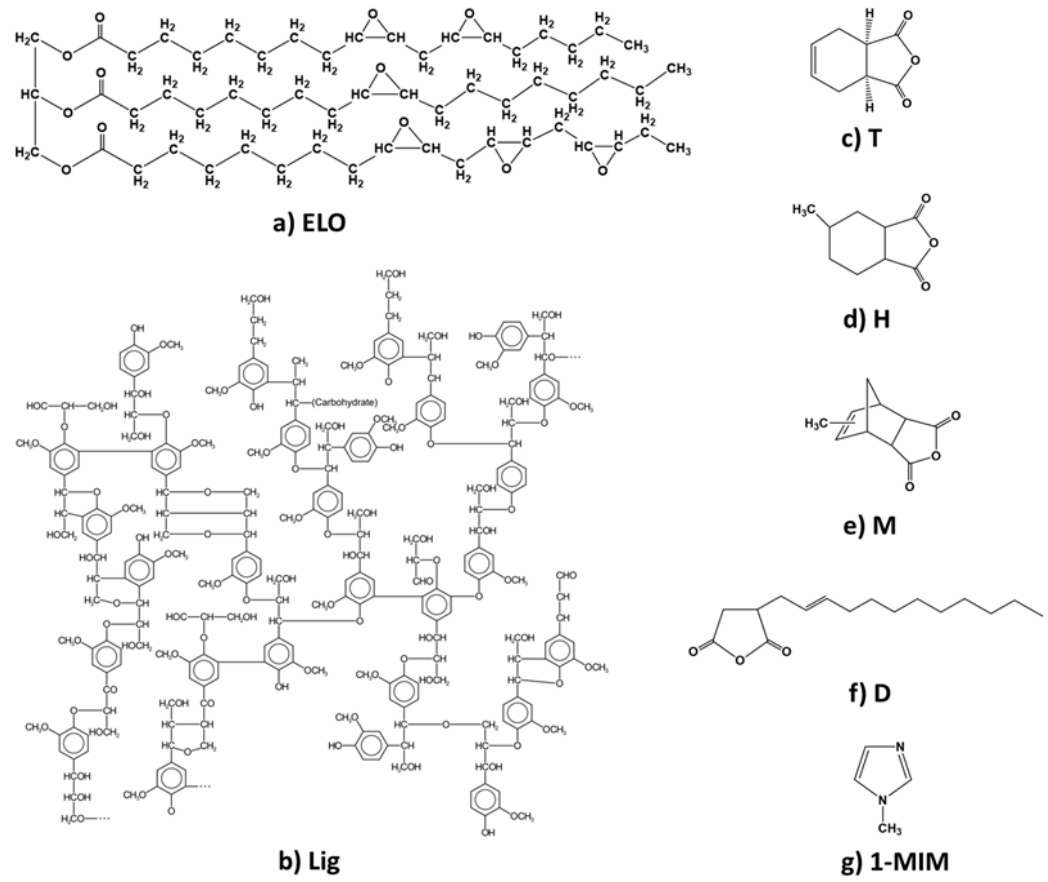

Figure 1: Chemical structure of: a) epoxidized linseed oil (ELO), b) Kraft lignin (Lig), c) cis-1,2,3,6-tetrahydrophthalic anhydride (T), d) hexahydro-4-methylphthalic anhydride (H), e) methyl nadic anhydride (M), f) (2-dodecen-1-yl)succinic anhydride (D) and g) 1-methylimidazole (1-MIM)

Gel content

The gel content (GC) of the materials was determined using the solvent extraction method. Samples with predetermined dimensions (20 × 8 × 4 mm^3) were initially weighed (W_0) and then immersed in acetone solvent at room temperature. The tested formulations were kept in solvent for 24 h, then removed and dried in the oven at 50 °C to a constant weight (W_d). The GC was calculated using the equation:[35]

$$GC, \% = 100 - \left[\frac{(W_0 - W_d) \times 100}{W_0}\right] \quad (2)$$

RESULTS AND DISCUSSION

Study of copolymerization reactivity by DSC

The dynamic curing behavior of the ELO monomer with different anhydrides, as well as the influence of lignin on this curing, was studied by DSC. Firstly, different initiator

types and concentrations were studied by DSC to find the best reactivity for the selected epoxy/anhydride systems (Fig. 2a). Based on the DSC results, 3 wt% of 1-MIM was selected as the optimal initiator and ratio due to the lowest maximum temperature and interval of reaction, and due to the high reaction enthalpy. Boquillon *et al.*[9] studied the influence of different anhydrides and initiators on the physico-chemical and mechanical properties of the ELO polymeric networks. After the kinetic investigations, they concluded that imidazole was more effective than the tertiary amines in the initiation of the polymerization, because the resulting networks showed a higher conversion of anhydride.

To determine the optimal amount of lignin that can be included in the epoxy/anhydride formulations, mass percentages of 5, 10, 15, 20, 30 and 40 wt% were tested. As an example, non-isothermal curing DSC curves of the ELO/(2-Dodecen-1-yl) succinic anhydride formulation with various lignin amounts are given in Figure 2b.

The curing reaction of ELO with (2-dodecen-1-yl) succinic anhydride (D) appears as a single broad exothermic event, with an exothermal shoulder at ~190 °C, a sign of secondary reactions, such as epoxy homopolymerization, etherification, *etc*. From Figure 2b, it can be seen that, with the addition of lignin, the peak of this secondary reaction decreases, disappearing for mixtures with 30 and 40 wt% lignin. The enthalpy of the epoxy/anhydride polymerization was determined by integrating the exothermic peak, while for the mixtures with lignin, the enthalpy values were normalized to the mass of the resin in the analyzed compositions. The influence of the Lig on the resins' reactivity can be observed from the modification of the T_{peak}, as well as of the reaction interval of temperature. As the percentage of lignin in the formulation increases, the T_{peak} value shifts to a lower temperature, except for the mixtures with 5 wt% Lig.

Generally, the T_{peak} temperature achieved from DSC curves is often taken as an indicator to assess the reactivity of the analyzed systems. According to previous studies,[36,37] it is known that the lower is the maximum temperature of the reaction, the higher is the reactivity. By DSC analysis and by the manufacturing protocol, it was established that the optimal and maximum amount of lignin to be added to the epoxy/anhydride systems is 30 wt%.

Figure 3 displays the DSC heating thermograms of ELO/anhydride curing systems with and without lignin, and the related data are summarized in Table 1. According to the obtained DSC data, the epoxy curing reactions of ELO/T, ELO/D and ELO/H exhibit similar T_{peak} values of about 150-153 °C, while the maximum temperature of reaction for the ELO/M is higher, being ~178 °C.

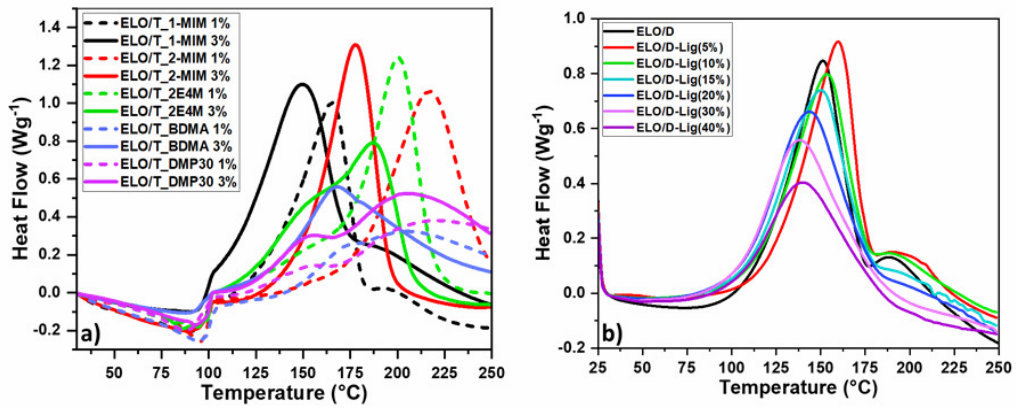

Figure 2: DSC curing during heating at 10 °C/min of a) ELO/cis-1,2,3,6-tetrahydrophthalic anhydride formulation initiated by 1 wt% (dot line) or 3 wt% (line) 1-methylimidazole (1-MIM, black curves), 2-methylimidazole (2-MIM, red curves), 2-ethyl-4-methylimidazole (2E4M, green curves), N,N-dimethylbenzylamine (BDMA, blue curves), 2,4,6-tris(dimethylaminomethyl)phenol (DMP30, purple curves), and b) ELO/ (2-dodecen-1-yl)succinic anhydride curing formulations with different percentages of lignin

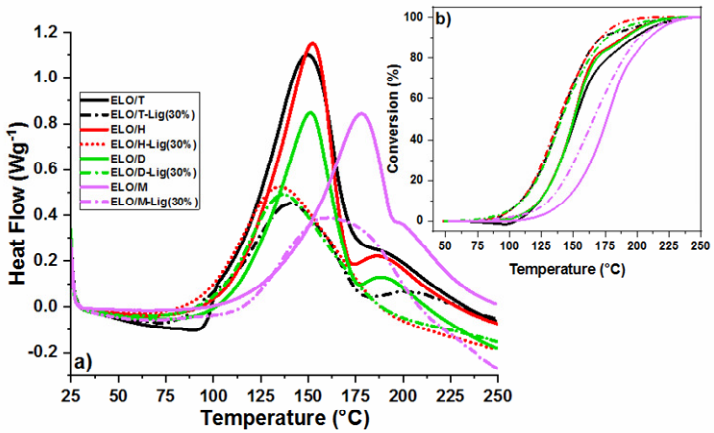

Figure 3: a) DSC curves of the curing process of the ELO/anhydride systems without and with 30 wt% lignin, and b) the conversion profile as a function of temperature

Table 1
DSC data of the curing process of ELO/anhydride formulations with and without 30 wt% lignin – reaction peak temperature, reaction interval of temperature and reaction enthalpy

DSC data	ELO/T		ELO/H		ELO/D		ELO/M	
	Resin	+30 wt% Lignin	Resin	+30 wt% Lignin	Resin	+30 wt% Lignin	Resin	+30 wt% Lignin
T_{peak} (°C)	150	140	153	136	151	137	178	164
(T_{onset} - T_{end}) (°C)	(90-250)	(73-250)	(73-250)	(64-225)	(78-250)	(55-220)	(86-250)	(68-250)
ΔH (J.g^{-1})	399	283	334	339	287	301	263	371

With the addition of 30 wt% lignin, the T_{onset} and T_{peak} decreased for all the studied systems, evidencing that this compound acts not only as filler, but also is involved as co-reactant in the crosslinking of the systems. In addition, the conversion of the reaction of the epoxy resins and composites was calculated by integrating the DSC thermograms with linear base approximation, the curve profiles being plotted as a function of the temperature in Figure 3b. Studying the conversion curves of the epoxy resins, it can be seen that the ELO/M reaction conversion occurs at higher temperature (110-240 °C), compared to the other three formulations (95-225 °C). The conversion profiles for the blends with lignin were restrained at lower temperature than those of neat resins. The curing reaction of the ELO/M-30%Lig started relatively slowly and reached a maximum reaction rate at around 165 °C, while for the other three epoxy composites, the maximum reaction rate ranges between 130-140 °C.

Therefore, considering the results obtained from the DSC analyses, it was established that 3 wt% 1-MIM represents the optimal initiator among those tested. Also, the ratio of 30 wt% lignin led to an improvement in the reactivity of the systems, demonstrating its contribution as co-reactant to epoxy/anhydride curing.

Thermal and mechanical characterization of thermosets and composites

The epoxy/anhydride and composites were studied by DMA, the measured storage modulus (*E*') being displayed in Figure 4. Studying the *E*' profile, we can identify the three stages, namely, the glassy plateau, the *α*-transition and the rubbery region. Corroborated with previously reported studies,[9,38,39] this work also confirms that the nature of the anhydride influences the thermomechanical properties of the developed epoxy polymeric network. The thermoset resins developed by crosslinking ELO with hexahydro-4-methylphthalic anhydride, cis-1,2,3,6-tetrahydrophthalic anhydride and methyl nadic anhydride revealed good and similar storage modulus in the glassy plateau (-30 °C), of about 2.1-2.4 GPa, while the system developed with (2-dodecen-1-yl)succinic anhydride has a twice lower *E*' value (1.1 GPa). Then, with increasing temperature, the *E*' value decreases significantly to a stable value, which indicates that the crosslinked networks are in a stable rubbery state.

The elastic response of the epoxy matrices reinforced with 30 wt% lignin was also studied. Comparing the DMA analysis data of the ELO/anhydride resins with those of the composites, the addition of lignin decreased the storage modulus of the developed networks, making them less brittle. The storage modulus of the resins in the rubbery region is proportional to the crosslink density (*v*) of the network, or inversely proportional to the molecular mass between crosslinks (M_c).

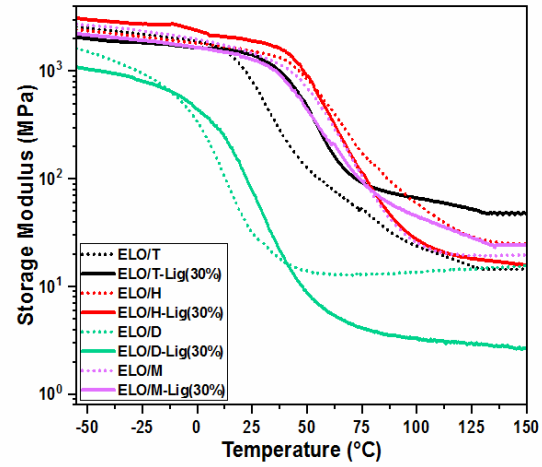

Figure 4: Storage modulus (E') curves of ELO/anhydride resins and composites with 30 wt% lignin

Table 2
Physical and thermomechanical properties of ELO/anhydride resins and composites with 30 wt% lignin

Sample	Density (g/cm^3)	Hardness test (SD)	E' in glassy region (-30 °C) (MPa)	Glass transition (°C)		υ (mmol·cm^{-3})	Mc (g/mol)	Gel content (%)
				T_g (DSC)	tan δ			
ELO/T	1.024	52	2259	25	41	2.04	721.02	99.45
ELO/T-Lig(30%)	0.867	65	1847	49	56	5.18	180.1	89.62
ELO/H	1.062	73	2139	58	75	2.40	392.93	97.74
ELO/H - Lig(30%)	1.031	71	2772	66	72	1.60	586.03	91.76
ELO/D	1.014	36	1064	12	21	1.46	680.98	98.67
ELO/D - Lig(30%)	1.035	44	882	18	34	0.34	3615.9	89.06
ELO/M	1.079	74	2439	62	75	1.87	562.02	99.81
ELO/M - Lig(30%)	0.803	65	1978	46	62	2.46	313.9	89.24

Using the DMA data, the crosslink density of the epoxy/anhydride resins and composites was calculated using the equation:[40]

$$\upsilon = \frac{E'}{3RT} \quad (3)$$

where E' represents the storage modulus in the rubbery plateau at T_g + 70 °C (MPa), R is the universal gas constant, and T is the absolute temperature (K).

The average molecular weight between crosslinks was also calculated based on the relationship established by Tobolsky:[41]

$$Mc = \frac{3\rho RT}{E'} \qquad Mc = \frac{\rho}{\vartheta} \quad (4)$$

where ρ is the calculated density (g.cm^{-3}) and E' is the storage modulus in the rubbery plateau (MPa) at 130 °C.

The variation of the anhydrides' chemical composition conducts to the development of polymeric networks with various mechanical behavior. The calculated values of υ and M_c are given in Table 2. Therefore, the increase of the crosslink density reduces chain mobility, making the networks more rigid. Moreover, the crosslink density of the materials is related to the amplitude of tan δ, so the higher is the peak amplitude, the more elastic is the material. The highest stiffness was obtained for ELO/H thermoset, followed by the other resins in the following order: ELO/T > ELO/M > ELO/D. The addition of lignin produces a two-fold increase of the crosslink density value in the case of ELO/T and ELO/M systems. In contrast, in the case of ELO/H and ELO/D thermosets, the υ values were reduced two or three times, respectively.

The damping factor (tan δ) is related to the cooperative chain motions and is associated with the macroscopic T_g of the thermoset materials. Figure 5 displays the temperature dependence of the loss factor tan δ for the analyzed thermosets and composites. The T_g values were determined by DSC and the obtained data are listed in Table 2. A comparison between the T_g values measured by DSC (under no mechanical stress) and the tan δ values measured by DMA under mechanical stress at a frequency of 1.0 Hz (based on the ASTM D7028 international standard)[42] is presented in Figure 6. The values recorded by the two techniques vary considerably due to the fact that the glass transition is a region between the states of thermodynamic equilibrium, being directly dependent on various physico-chemical and mechanical factors.[43,44] According to Figure 5, the most elastic epoxy resin is ELO/D, presenting a tan δ at ~21 °C. As a function of the anhydride nature, the glass transition increases considerably, reaching ~75 °C for the systems with hexahydro-4-methylphthalic anhydride or methyl nadic anhydride. The addition of lignin led either to the stiffening of the thermosets or to their plastification. For example, the tan δ values of ELO/T and ELO/D composites increased with ~13-15 °C, the lignin increasing the rigidity of materials. For ELO/H and ELO/M systems, the tan δ

values decreased by around 3 °C and 13 °C, respectively, the lignin acting here as a plasticizer, thus reducing the fragile character of the epoxy resins. A similar trend was also revealed by the rigidity values (Table 2) of the materials obtained by Shore D hardness test. The obtained stiffness values for the thermosets and composites range between 36 SD and 74 SD. According to the Shore D scale, these materials belong to medium hard (*e.g.* door seal, automotive tire tread) to extra hard materials (*e.g.* solid truck tires, hard wheels). Based on previous studies,[10] this behavior is related to the structure of the materials and the amount of chemical connections developed in the networks.

The gel content values obtained for the four ELO-based resins and composites are listed in Table 2. We can highlight that all the ELO/anhydride thermosets exhibit a high GC%, between 97.74% and 99.81%, indicating that ELO is well cured by the four different anhydrides. Values higher than 99% indicate that no free species remain in the analyzed network and the crosslinking of these systems is complete. In the case of the epoxy resins reinforced with 30 wt% lignin, a slight decrease in gel content values can be observed, varying between 89% and 91.76%. These lower values of the GC% for composites can be caused by the unlinked lignin present in the materials composition. With the immersion into acetone of the composites, the chemically unbound lignin particles were dislocated from the material's structure, being released into the solvent, thus leading to the formation of free spaces in the polymeric network.

Thermal stability studies

Figure 7 presents the TGA analysis under oxidative atmosphere of the ELO/anhydride polymeric resins and their composites with 30 wt% Lig. The degradation temperature ($T_{5\%}$) of the materials and the temperature corresponding to the maximum decomposition rate (T_{dmax}) were recorded from the TGA/DTG data and listed in Table 3, together with the statistic heat-resistance index (T_s). The T_s factor represents the temperature of the polymers in the physical heat tolerance limit and was calculated using the equation:[37,45–47]

$$T_s = 0.49\left[T_{5\%} + 0.6\left(T_{30\%} - T_{5\%}\right)\right] \quad (5)$$

where the $T_{30\%}$ is the temperature at which the analyzed materials lose 30% of their mass.

The obtained data show that the cured epoxy/anhydride resins are generally thermally stable up to 300 °C, excepting the system with methyl nadic anhydride, which presents a $T_{5\%}$ at ~284 °C. This minor difference in thermal stability between the systems demonstrates that the anhydride nature does not significantly influence the thermal behavior of the polymeric materials, which was also highlighted by Gerbase *et al.*[38]

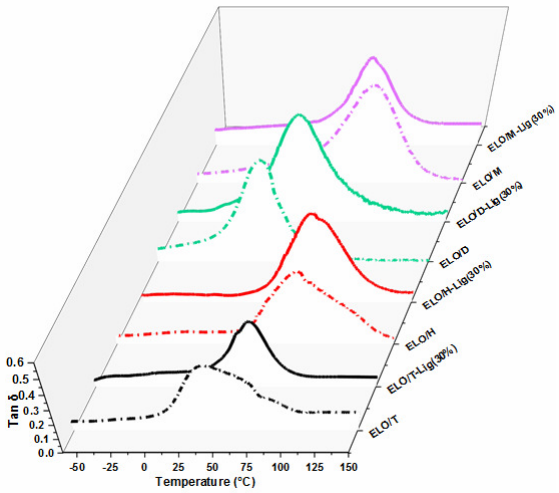

Figure 5: Temperature dependence of loss factor tan δ for the ELO/anhydride thermosets and composites

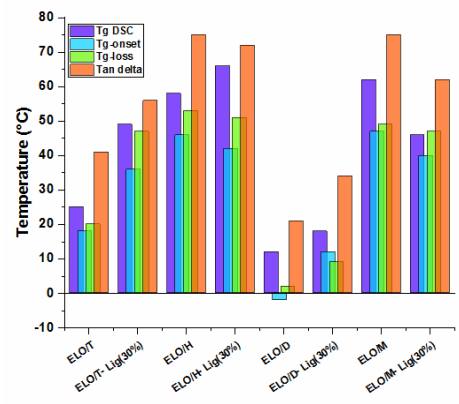

Figure 6: Glass transition temperatures for the epoxy thermoset resins and composites determined by DSC and DMA

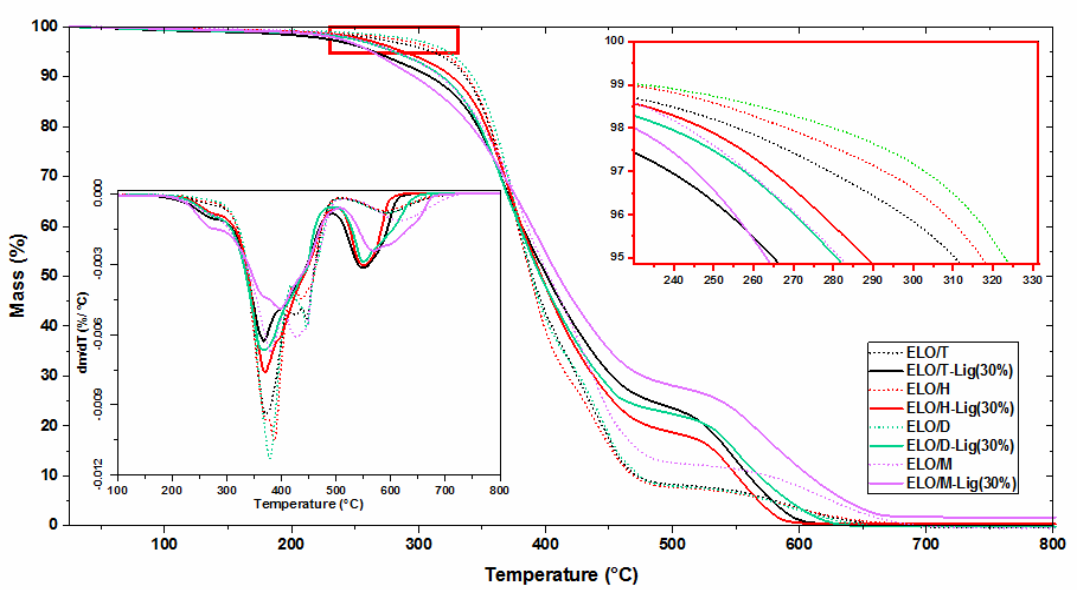

Figure 7: TGA and DTG (bottom left corner) curves as a function of temperature for resins and composites, heating at 10 °C/min, under air flow

Table 3
TGA/DTG results for resins and composites analysis

Sample	$T_{5\%}$ (°C)	T_{dmax} (°C)	T_s (°C)
ELO/T	310	370	170
ELO/T-Lig(30%)	270	370	160
ELO/H	320	389	171
ELO/H-Lig(30%)	290	370	165
ELO/D	320	380	172
ELO/D-Lig(30%)	282	369	163
ELO/M	284	379	164
ELO/M-Lig(30%)	264	399	161

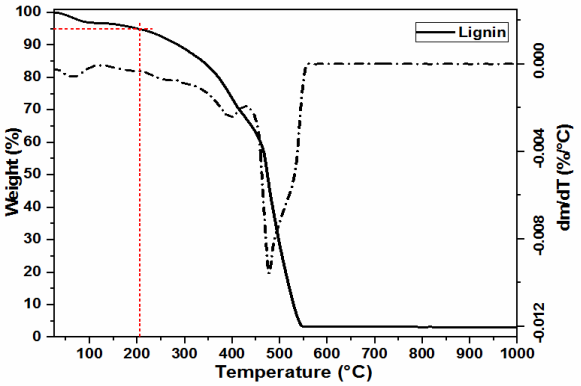

Figure 8: TGA/DTG curve versus temperature for the raw Kraft lignin

The addition of lignin led to a slight diminution in the thermal stability of the composites, still remaining very good, above 265 °C. This result may be due to the thermal stability of the raw lignin ($T_{5\%}$ = 202 °C) (Fig. 8).

Studying the DTG curves, we can observe the presence of two complex and major inflection points for all the epoxy resins and composites. Before the first major degradation step, a slight decomposition shoulder between 200-280 °C can be observed for all the

developed materials. This first small step can be attributed to the volatilization of the adsorbed water, which in the case of the composites overlaps with the beginning of the thermal decomposition of lignin.[48–50] The first step represents the main thermal degradation stage for both the resins and the composites. This decomposition stage appears as a large and complex exothermic peak ranging between 300 °C and up to 510 °C, with a maximum at about 370-400 °C (T_{dmax}, Table 3), and is associated with the thermolysis of the polymer structure. In the case of the epoxy resins, the mass loss in this step is about 80-89%, this percentage varying depending on the anhydride nature in the order: ELO/M < ELO/D < ELO/T < ELO/H. Likewise, it was observed that, although the addition of lignin reduced the $T_{5\%}$ values of the composites, their mass loss percentage in the first main step decreased considerably, compared to the neat resins, being about 58-73%. The second degradation stage, of thermo-oxidative degradation and carbonization of the resins and composites, appears in the DTG thermograms (Fig. 7) as a well-defined exothermic peak ranging between 500-750 °C. At this stage, the mass loss of the epoxy resins is about 7-13%, while for the related composites filled with 30 wt% lignin, the mass loss percentage ranges from 18 up to 26%.

Water absorption

The water absorption of the prepared materials was evaluated using two different techniques: by the ASTM D570 method and by the DSC method. The water uptake evolution of the epoxy resins and composites after 24 h of immersion is displayed in Figure 9. The water absorption of materials is influenced by various factors, as for example, the existence of microcracks and pores, which are present in some epoxy resins.[51–54] Another factor that influences the water absorption is the presence of free hydroxyl or other polar groups, which can increase the WA by hydrogen bonding.[55] The water gain in the neat epoxy polymers, after 24 h of immersion, ranged between 0.6% and 1.2%, depending on the anhydride nature. Studying the obtained WA results and comparing them with the calculated crosslink density (Table 2), it can be observed that the lower is the crosslink density, the higher is the WA. So, the moisture uptake values of the epoxy/anhydride resins are in the following order: ELO/D > ELO/M > ELO/T > ELO/H.

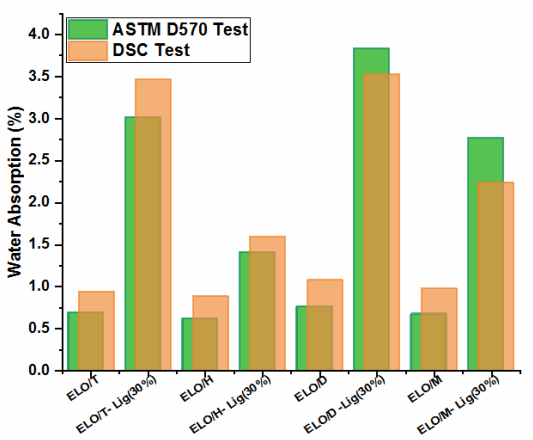

Figure 9: WA% after 24 h of immersion: comparison between ASTM D570 standard test and DSC test

The addition of 30 wt% lignin increased 2-4-fold the WA values of the composites. Lignocellulose fibers are highly hydrophilic due to the presence of -OH groups, permitting moisture absorption by hydrogen bonding.[53] From Figure 9, we can notice that even if the amount of WA increases with the addition of lignin, it still remains relatively low, between 1.4-3.7%. We have already shown that the presence of filler in the composites interferes

with the curing process of the matrix, leading to a decrease in the crosslinking of the matrix, which facilitates the penetration of water into the polymer network. The decrease of composites' WA can be achieved using adequate coatings or fiber treatment.[56]

CONCLUSION

Epoxidized linseed oil was copolymerized with various anhydrides, such as cis-1,2,3,6-tetrahydrophthalic anhydride, hexahydro-4-methylphthalic anhydride, (2-dodecen-1-yl)succinic anhydride and methyl nadic anhydride, the reactions being initiated by 1-methylimidazole. Afterwards, the designed epoxy/anhydride resins were reinforced with a very high amount (30 wt%) of a natural derived raw material, namely lignin. The reactivity of the resins and the influence of the filler on the curing process were investigated by the DSC technique. DSC analyses showed that the copolymerization reaction was improved in the presence of lignin, by decreasing the reaction temperature interval and T_{peak}.

The variation of the anhydride chemical nature led to the development of materials with modular properties. The tan δ values of the ELO-based resins ranged between 21 °C and 75 °C, the materials varying from elastic to rigid. The addition of lignin modified differently the mechanical properties of the composites, depending on the nature of the polymer matrix; for the systems ELO/T and ELO/D, the lignin acted as a filler, imparting rigidity to the materials, while for the systems ELO/H and ELO/M, the lignin acted as a plasticizer, reducing the brittle character of the resins and making the materials more ductile.

Based on the Shore D hardness test, the obtained resins and composites are classified into the medium hard to extra hard material category, with values from 36 SD up to 74 SD. Moreover, the synthesized polymeric materials revealed very low water absorption, with values between 0.6-1.2% for the resins and 1.4-3.7% for the composites with lignin. These materials also showed high gel content, being over 98% for the resins and ~89-92% for the composites.

In conclusion, in this work, various polymeric materials were synthesized with good physico-chemical, thermal and thermo-mechanical properties. The lignin that was used in very large quantities played the role of both a co-macromonomer and a filler, thus leading to the development of new polymer networks. These thermosets with high biobased content have the potential to substitute some petroleum-based polymers in applications such as automotive parts, composites, semi-manufactured products, *etc*.

ACKNOWLEDGMENT: This work was supported by ECOXY project. ECOXY is a project funded by the European Commission. This project has received funding from the Bio Based Industries Joint Undertaking under the European Union's Horizon 2020 research and innovation program (Grant agreement n° 744311).

REFERENCES

[1] D. Hosler, *Science*, **284**, 1988 (1999), https://doi.org/10.1126/science.284.5422.1988
[2] A. Okunola, I. O. Kehinde, A. Oluwaseun and E. A. Olufiropo, *J. Toxicol. Risk Assess.*, **5**, 021 (2019), https://doi.org/10.23937/2572-4061.1510021
[3] B. Kamm, P. R. Gruber and M. Kamm, "Biorefineries-Industrial Processes and Products. Status Quo and Future Directions", Wiley-VCH Verlag GmbH & Co. KGaA, Weinheim, 2006, vol. 1, https://doi.org/10.1002/9783527619849.ch22
[4] G. Mashouf Roudsari, A. K. Mohanty and M. Misra, *ACS Sustain. Chem. Eng.*, **5**, 9528 (2017), https://doi.org/10.1021/acssuschemeng.7b01422
[5] E. Ramon, C. Sguazzo and P. Moreira, *Aerospace*, **5**, 110 (2018), https://doi.org/10.3390/aerospace5040110
[6] J.-P. Pascault and R. J. Williams, "Epoxy Polymers-New Materials and Innovations", Wiley-VCH Verlag GmbH & Co. KGaA, 2010
[7] Y. Xia and R. C. Larock, *Green Chem.*, **12**, 1893 (2010), https://doi.org/10.1039/c0gc00264j
[8] N. B. Samarth and P. A. Mahanwar, *Open J. Org. Polym. Mater.*, **05**, 1 (2015), https://doi.org/10.4236/ojopm.2015.51001
[9] N. Boquillon and C. Fringant, *Polymer (Guildf)*, **41**, 8603 (2000), https://doi.org/10.1016/S0032-3861(00)00256-1
[10] M. D. Samper, V. Fombuena, T. Boronat, D. García-Sanoguera and R. Balart, *J. Am. Oil Chem. Soc.*, **89**, 1521 (2012), https://doi.org/10.1007/s11746-012-2041-y
[11] C. Di Mauro, A. Genua and A. Mija, *Mater. Adv.*, **1**, 1788 (2020), https://doi.org/10.1039/D0MA00370K
[12] C. Di Mauro, T.-N. Tran, A. Graillot and A. Mija, *ACS Sustain. Chem. Eng.*, **8**, 7690 (2020), https://doi.org/10.1021/acssuschemeng.0c01419

[13] C. Di Mauro, S. Malburet, A. Genua, A. Graillot and A. Mija, *Biomacromolecules*, **21**, 3923 (2020), https://doi.org/10.1021/acs.biomac.0c01059
[14] D. J. Morris and I. Ahmed, "The Carbohydrate Economy: Making Chemicals and Industrial Materials from Plant Matter", Institute for Local Self-Reliance, 1992
[15] R. Wool and X. S. Sun, "Bio-Based Polymers and Composites", 1st ed., Elsevier, 2005
[16] S. N. Khot, J. J. Lascala, E. Can, S. S. Morye, G. I. Williams *et al*., *J. Appl. Polym. Sci*., **82**, 703 (2001), https://doi.org/10.1002/app.1897
[17] I. Delidovich, P. J. C. Hausoul, L. Deng, R. Pfützenreuter, M. Rose *et al*., *Chem. Rev*., **116**, 1540 (2016), https://doi.org/10.1021/acs.chemrev.5b00354
[18] A. Barakat, H. de Vries and X. Rouau, *Bioresour. Technol*., **134**, 362 (2013), https://doi.org/10.1016/j.biortech.2013.01.169
[19] M. Taherzadeh and K. Karimi, *Int. J. Mol. Sci*., **9**, 1621 (2008), https://doi.org/10.3390/ijms9091621
[20] V. K. Ponnusamy, D. D. Nguyen, J. Dharmaraja, S. Shobana, J. R. Banu *et al*., *Bioresour. Technol*., **271**, 462 (2019), https://doi.org/10.1016/j.biortech.2018.09.070
[21] A. Ház, M. Jablonský, I. Šurina, F. Kačík, T. Bubeníková *et al*., *Forests*, **10**, 483 (2019), https://doi.org/10.3390/f10060483
[22] J. H. Lora and W. G. Glasser, *J. Polym. Environ*., **10**, 39 (2002), https://doi.org/10.1023/A:1021070006895
[23] O. A. T. Dias, D. R. Negrão, R. C. Silva, C. S. Funari, I. Cesarino *et al*., *Mol. Cryst. Liq. Cryst*., **628**, 72 (2016), https://doi.org/10.1080/15421406.2015.1137677
[24] O. A. T. Dias, M. Sain, I. Cesarino and A. L. Leão, *Polym. Adv. Technol*., **30**, 70 (2019), https://doi.org/10.1002/pat.4444
[25] M. A. S. Anwer, H. E. Naguib, A. Celzard and V. Fierro, *Compos. Part B Eng*., **82**, 92 (2015), https://doi.org/10.1016/j.compositesb.2015.08.028
[26] O. Gordobil, R. Delucis, I. Egüés and J. Labidi, *Ind. Crop. Prod*., **72**, 46 (2015), https://doi.org/10.1016/j.indcrop.2015.01.055
[27] Q. Ping, J. Xiao and J. Zhao, *Adv. Mater. Res*., **236–238**, 1195 (2011), https://doi.org/10.4028/www.scientific.net/AMR.236-238.1195
[28] J. Sun, C. Wang, J. C. C. Yeo, D. Yuan, H. Li *et al*., *Macromol. Mater. Eng*., **301**, 328 (2016), https://doi.org/10.1002/mame.201500310
[29] Q. Yin, W. Yang, C. Sun and M. Di, *BioResources*, **7**, 5737 (2012), https://doi.org/10.15376/biores.7.4.5737-5748
[30] M. Fache, B. Boutevin and S. Caillol, *Green Chem*., **18**, 712 (2016), https://doi.org/10.1039/c5gc01070e
[31] F. Ferdosian, Z. Yuan, M. Anderson and C. Xu, *Thermochim. Acta*, **618**, 48 (2015), https://doi.org/10.1016/j.tca.2015.09.012
[32] R. Dinu, C. Cantarutti and A. Mija, *ACS Sustain. Chem. Eng*., **8**, 6844 (2020), https://doi.org/10.1021/acssuschemeng.0c01759
[33] R. Dinu and A. Mija, *J. Mater. Sci. Res*., **9**, 183 (2020)
[34] ASTM-D570, Water Absorption of Plastics, 1998, https://doi.org/10.1520/D0570-98
[35] S. G. Tan, Z. Ahmad and W. S. Chow, *Polym. Int*., **63**, 273 (2014), https://doi.org/10.1002/pi.4501
[36] X. Liu, W. Xin and J. Zhang, *Green Chem*., **11**, 1018 (2009), https://doi.org/10.1039/b903955d
[37] S. Ma, X. Liu, L. Fan, Y. Jiang, L. Cao *et al*., *ChemSusChem*, **7**, 555 (2014), https://doi.org/10.1002/cssc.201300749
[38] A. E. Gerbase, C. L. Petzhold and A. P. O. Costa, *J. Am. Oil Chem. Soc*., **79**, 797 (2002), https://doi.org/10.1007/s11746-002-0561-z
[39] H. Miyagawa, A. K. Mohanty, M. Misra and L. T. Drzal, *Macromol. Mater. Eng*., **289**, 629 (2004), https://doi.org/10.1002/mame.200400004
[40] P. J. Flory, "Principles of Polymer Chemistry", Cornell University Press, 1953
[41] A. V. Tobolsky, "Properties and Structure of Polymers", Wiley, New York, 1960
[42] ASTM-D7028, Standard Test Method for Glass Transition Temperature (DMA Tg) of Polymer Matrix Composites by Dynamic Mechanical Analysis (DMA), 2008, https://doi.org/10.1520/D7028-07E01.2
[43] M. Fache, A. Viola, R. Auvergne, B. Boutevin and S. Caillol, *Eur. Polym. J*., **68**, 526 (2015), https://doi.org/10.1016/j.eurpolymj.2015.03.048
[44] I. M. Kalogeras and H. E. Hagg Lobland, *J. Mater. Educ*., **34**, 69 (2012)
[45] C. Aouf, H. Nouailhas, M. Fache, S. Caillol, B. Boutevin *et al*., *Eur. Polym. J*., **49**, 1185 (2013), https://doi.org/10.1016/j.eurpolymj.2012.11.025
[46] H. Nouailhas, C. Aouf, C. Le Guerneve, S. Caillol, B. Boutevin *et al*., *J. Polym. Sci. Part A Polym. Chem*., **49**, 2261 (2011), https://doi.org/10.1002/pola.24659
[47] S. Ma, C. S. Kovash and D. C. Webster, *J. Coatings Technol. Res*., **14**, 367 (2017), https://doi.org/10.1007/s11998-016-9863-8
[48] S. Hirose, T. Hatakeyama and H. Hatakeyama, *Procedia Chem*., **4**, 26 (2012), https://doi.org/10.1016/j.proche.2012.06.004
[49] T. Väisänen, O. Das and L. Tomppo, *J. Clean. Prod*., **149**, 582 (2017), https://doi.org/10.1016/j.jclepro.2017.02.132
[50] P. Liminana, D. Garcia-Sanoguera, L. Quiles-Carrillo, R. Balart and N. Montanes, *Compos. Part B Eng*., **144**, 153 (2018), https://doi.org/10.1016/j.compositesb.2018.02.031

[51] A. Moudood, A. Rahman, A. Öchsner, M. Islam and G. Francucci, *J. Reinf. Plast. Compos.*, **38**, 323 (2019), https://doi.org/10.1177/0731684418818893
[52] M. Assarar, D. Scida, A. El Mahi, C. Poilâne and R. Ayad, *Mater. Des.*, **32**, 788 (2011), https://doi.org/10.1016/j.matdes.2010.07.024
[53] A. Moudood, A. Rahman, H. M. Khanlou, W. Hall, A. Öchsner *et al.*, *Compos. Part B Eng.*, **171**, 284 (2019), https://doi.org/10.1016/j.compositesb.2019.05.032
[54] E. Muñoz and J. A. García-Manrique, *Int. J. Polym. Sci.*, **2015**, 1 (2015), https://doi.org/10.1155/2015/390275
[55] G. Capiel, J. Uicich, D. Fasce and P. E Montemartini, *Polym. Degrad. Stabil.*, **153**, 165 (2018), https://doi.org/10.1016/j.polymdegradstab.2018.04.030
[56] F. Ahmad, H. S. Choi and M. K. Park, *Macromol. Mater. Eng.*, **300**, 10 (2015), https://doi.org/10.1002/mame.201400089